1550-nm Superprism Demultiplexers in 2-D Silicon-on-Insulator Slabs

Jin Yao, Ming-Chang M. Lee and Ming C. Wu
Dept. Electrical Engineering, University of California, Los Angeles, CA90095, USA
Email: jinyao@ucla.edu

Abstract: Superprism phenomena are demonstrated in the 1550nm range with SOI-based 2D photonic crystal slab. An angular swing of up to 10° is observed as the input wavelength is changed from 1528 nm to 1557 nm.

OCIS codes: (130.3120) Integrated optics devices; (060.1810) Coupler, switches, and multiplexers

1. Introduction

Photonic crystals (PCs) are promising for realizing ultra-compact wavelength-division multiplexing (WDM) components because of their ability to control light propagation on a wavelength scale. One of the extraordinary properties of PC is the "superprism" phenomena. In the vicinity of the photonic bandgap, the propagation direction of light becomes super sensitive to its wavelength and incident angle.

The prism function in PC was first reported by Lin *et al.* in millimeter-wave frequencies [1]. Recently, Kosaka *et al.* demonstrated the superprism phenomena in 3-D PCs at 1-μm wavelength [2,3]. Their structures showed 50 times stronger dispersion than that in [1], or about 500 times larger than that of a conventional prism. However, the 3-D PC realized by multilayer deposition on patterned substrate (autocloning) is essentially a bulk optical element and is difficult to integrate with other photonic elements [4]. On the other hand, 2-D PCs also exhibit superprism phenomena. They have simpler fabrication process and are compatible with planar lightwave integrated circuits. Using GaAs-based 2-D PCs, a dispersion of 0.5°/nm has been reported for wavelengths from 1290 to 1310 nm [5,6].

In this paper, we report on the first superprism in the 1550-nm range using silicon-on-insulator (SOI) 2-D PCs. An angular dispersion of 0.34°/nm (10° shift for wavelength from 1528 to 1557 nm) has been experimentally achieved. Integration with waveguides is also demonstrated.

2. Design, fabrication, and measurement setup

Our photonic crystal slab is fabricated on a SOI substrate with a 270-nm-thick silicon layer and a 1-μm-thick buried oxide. The scanning electron micrograph (SEM) of the superprism test structure is shown in Fig. 1(a). The PC superprism has a semicircular shape with a radius of 24 μm. We employ PCs with hexagonal lattice and air holes. The lattice constant, a, is 670 nm and the hole radius, r, is 153 nm, as showed in Fig. 1(b). The output waveguides are arranged in a radial configuration with receiving angles from -80° to +80° (with increment of 10°). This configuration ensures the output light is perpendicular to interface of the PC area. To allow more experimental flexibility in the incident angle, the input waveguide is not integrated on the chip. Instead, the superprism chip is cleaved along the flat edge of the superprism, which is parallel to the Γ-K direction, as shown in Fig. 1(a). We use a wedge-shaped cylindrical lensed fiber to couple directly to the superprism. Incident angle can be varied by rotating the input fiber.

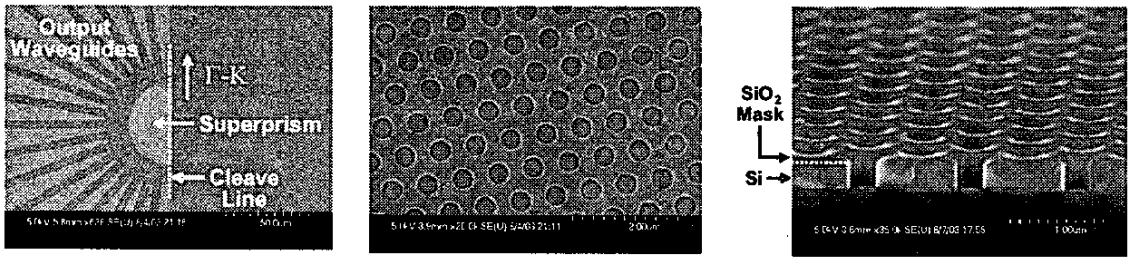

(a) (b) (c)

Fig. 1 SEM pictures of fabricated photonic crystal superprism: (a) semicircular PC superprism and surrounding output waveguides, (b) top view of the hexagonal PC lattice, and (c) cross-sectional profile showing the straight and smooth sidewalls.

The superprism test structure is fabricated by combining electron-beam (e-beam) and optical lithography. The fabrication process is summarized in the following: first, a 150-nm-thick layer of SiO_2 is deposited on top of the structure as the etching mask. Using a Leica EBL100 E-beam Writer, the photonic crystal pattern is written onto a 200-nm-thick Polymethylmethacylate (PMMA) resist. The pattern is transferred to the SiO_2 mask with CHF_3 chemical dry etching. The optical waveguides are patterned by optical lithography. To produce smooth vertical sidewalls, a chlorine-based inductively coupled plasma (ICP) etching is used to etch through the core Si layer. The final structure profile is showed as Fig. 1(c). Smooth and straight sidewalls are obtained without any footing (undercut near the bottom).

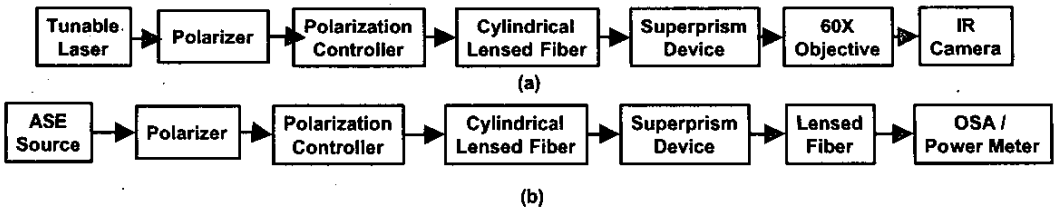

Fig. 2. Schematic measurement setup with (a) a tunable laser source and an IR camera and (b) an ASE source and an optical spectrum analyzer (OSA) and a power meter.

The schematic measurement setup is showed in Fig. 2. A C-band tunable laser source is employed to measure the angular power distribution at various wavelengths (Fig. 2(a)), while a broadband amplified spontaneous emission (ASE) source is used to measure the spectral response of various waveguides (Fig. 2(b)). A polarizer and a polarization controller are used to control the input polarization. The near-field profiles from the waveguides are imaged through a 60x objective lens to an IR camera in Fig. 2(a). The receiving fiber in Fig. 2(b) is a spherical lensed fiber.

3. Results and discussions

The input beam from the lens fiber is tilted 12° from the normal of the PC interface (Γ-M direction). The output light beams from the waveguides are imaged by the IR camera as the laser wavelength is tuned. The images in Fig. 3 show that the output light swings from the -70° waveguide to the -60° waveguide when the wavelength changes from 1557 nm to 1528 nm. The minus sign "-" here indicates the output waveguides are on the same side as the incident light with respect to the normal of the interface.

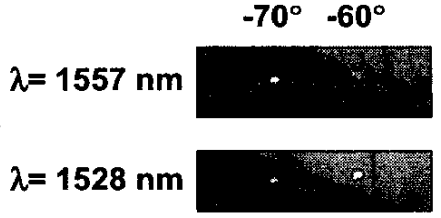

Fig. 3. IR images of the output waveguides at -70° and -60° for input wavelengths of 1557 and 1528 nm, respectively.

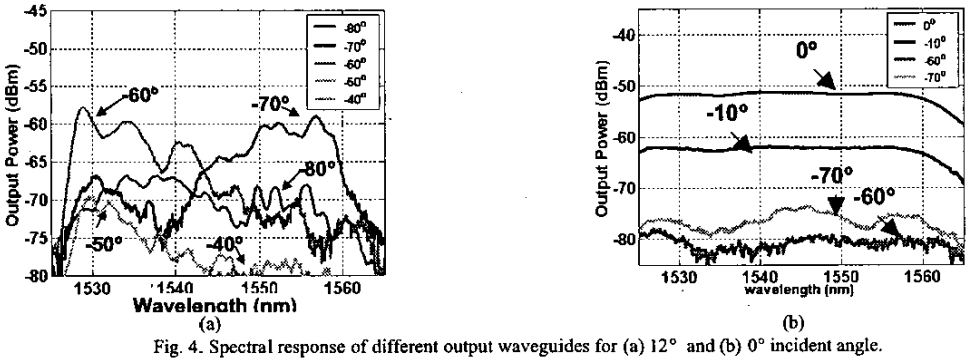

Fig. 4. Spectral response of different output waveguides for (a) 12° and (b) 0° incident angle.

The spectral response of the light from various output waveguides are shown in Fig. 4(a). The -70° and -60° waveguides have significantly higher output power than other waveguides. The peak wavelength for the -60° waveguide is 1528 nm and that of the -70° waveguide is 1557 nm. The resulting dispersion is 0.34°/nm. This agrees with the IR image results in Fig. 3. For comparison, we also measured the power distribution and the spectral response of the superprism at normal incidence, as shown in Fig. 4(b). Most of the power is directed towards the 0° waveguide. The spectral response is essentially flat from 1528 to 1560 nm. This confirms the superprism result in Fig. 4(a).

To quantify the efficiency of the superprism, we also fabricated a straight waveguide with similar length but without superprism. We compare the power from the output waveguide of the superprism and that of the straight waveguide. The calibrated transmittance response of the superprism is shown in Fig. 5. The efficiency is found to be approximately 0.31% at 1528 nm. The sources of losses include coupling into the leaky modes in this high-index-contrast 2-D slab, scattering from sample imperfections and sidewall roughness, and reflections at the interface between the PC and the slab areas. One of the possible ways to reduce the reflection loss is to introduce a graded input interface as an index matching region and an extended output to suppress diffracted waves [7, 8].

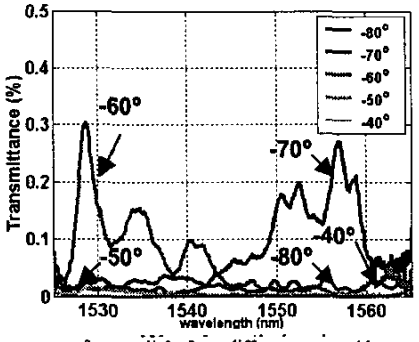

Fig.5. Transmittance spectra of output light from different waveguides at normal incidence.

The physical mechanism underlying these phenomena can by explained by dispersion surfaces constructed from photonic band structure. Specific modeling and detailed theoretical analysis will be expatiated in a separate paper. Although we only utilized the input interface to demonstrate the superprism phenomena, the overall device dispersion could be further magnified by utilizing the output interface refraction, as calculated and simulated in [8].

4. Conclusion

We have presented the first experimental results of a photonic crystal superprism in the 1550-nm wavelength range. A hexagonal photonic crystal with a lattice constant of 670 nm and a hole radius of 153 nm has been fabricated on a silicon-on-insulator (SOI) planar lightwave circuit (PLC). An angular swing of 10° is observed as the input wavelength changes from 1528nm to 1557nm, yielding a dispersion of 0.34°/nm. The combination of superprism and PLC can drastically reduce the size of future WDM components.

This project is supported by DARPA CS-WDM program under MDA972-02-1-0020.

5. Reference

[1] S. Y. Lin, V. M. Hietala, L. Wang, and E. D. Jones, "Highly dispersive photonic band-gap prism," Opt. Lett. **21**, 1771–1773, (1996).

[2] H. Kosaka, T. Kawashima, A. Tomita, M. Notomi, T. Tamamura, T. Sato, and S. Kawakami, "Superprism phenomena in photonic crystals," Phys. Rev. B, Condens.Matter **58**, 10 096–10 099, (1998).

[3] H. Kosaka, T. Kawashima, A. Tomita, M. Notomi, T. Tamamura, T. Sato, and S. Kawakami, "Superprism phenomena in photonic crystals: Toward microscale lightwave circuits," J. Lightwave Technol., **17**, 2032–2038, (1999).

[4] S. Kawakami, "Fabrication of submicrometer 3-D periodic structures composed of Si/SiO2," Electron. Lett., **33**, 1260–1261, (1997).

[5] L. Wu, M. Mazilu, T. Karle, and T. Krauss, "Superprism phenomena in planar photonic crystals," J. Quantum Electron., **38**, 915–918, (2002).

[6] L. Wu, M. Mazilu, T. Karle, and T. Krauss, "Beam Steering in Planar-Photonic Crystals: From Superprism to Supercollimator", J. Lightwave Technol. **21**, 561-566, (2003).

[7] T. Baba and D. Ohsaki, "Interfaces of photonic crystals for high efficiency light transmission," Jpn. J. Appl. Phys., pt. 1, **40**, 5920–5924, (2001).

[8] T. Baba and M. Nakamura, "Photonic Crystal Light Deflection Devices Using the Superprism Effect", J. Quantum Electron. **38**, 909-914, (2002)